RNA Biology 11:2, 146–155; February 2014; © 2014 Landes Bioscience

Crosslinking-immunoprecipitation (iCLIP) analysis reveals global regulatory roles of hnRNP L

Oliver Rossbach[1], Lee-Hsueh Hung[1], Ekaterina Khrameeva[2,3], Silke Schreiner[1], Julian König[4,5], Tomaž Curk[6], Blaž Zupan[6], Jernej Ule[5], Mikhail S Gelfand[2,3], and Albrecht Bindereif[1,*]

[1]Institute of Biochemistry; University of Giessen; Giessen, Germany; [2]Kharkevich Institute for Information Transmission Problems; Russian Academy of Sciences; Moscow, Russia; [3]Department of Bioengineering and Bioinformatics; Lomonosov Moscow State University; Moscow, Russia; [4]Institute of Molecular Biology (IMB); Mainz, Germany; [5]Institute of Neurology; University College London; London, United Kingdom; [6]Faculty of Computer and Information Science; University of Ljubljana; Ljubljana, Slovenia

Keywords: hnRNP L, CLIP, splicing regulation, microRNA

Heterogeneous nuclear ribonucleoprotein L (hnRNP L) is a multifunctional RNA-binding protein that is involved in many different processes, such as regulation of transcription, translation, and RNA stability. We have previously characterized hnRNP L as a global regulator of alternative splicing, binding to CA-repeat, and CA-rich RNA elements. Interestingly, hnRNP L can both activate and repress splicing of alternative exons, but the precise mechanism of hnRNP L-mediated splicing regulation remained unclear. To analyze activities of hnRNP L on a genome-wide level, we performed individual-nucleotide resolution crosslinking-immunoprecipitation in combination with deep-sequencing (iCLIP-Seq). Sequence analysis of the iCLIP crosslink sites showed significant enrichment of C/A motifs, which perfectly agrees with the in vitro binding consensus obtained earlier by a SELEX approach, indicating that in vivo hnRNP L binding targets are mainly determined by the RNA-binding activity of the protein. Genome-wide mapping of hnRNP L binding revealed that the protein preferably binds to introns and 3′ UTR. Additionally, position-dependent splicing regulation by hnRNP L was demonstrated: The protein represses splicing when bound to intronic regions upstream of alternative exons, and in contrast, activates splicing when bound to the downstream intron. These findings shed light on the longstanding question of differential hnRNP L-mediated splicing regulation. Finally, regarding 3′ UTR binding, hnRNP L binding preferentially overlaps with predicted microRNA target sites, indicating global competition between hnRNP L and microRNA binding. Translational regulation by hnRNP L was validated for a subset of predicted target 3′UTRs.

Introduction

The heterogeneous nuclear ribonucleoprotein L (hnRNP L) is a multifunctional RNA-binding protein containing four RNA-recognition motifs (RRMs), which specifically recognizes CA-repeat and CA-rich RNA elements.[1] It participates in diverse functions of mRNA metabolism, such as export of intronless mRNA,[2,3] translational regulation,[4-7] regulation of mRNA stability,[1,4,8,9] poly(A) site selection,[10] and alternative splicing.[10] Recent work by Jafarifar et al.[11] demonstrated yet another role: competing with microRNAs (miRNAs) for binding to a CA-rich RNA element within the *VEGFA* 3′ UTR. A similar mechanism was also very recently described for DGK-α.[12]

HnRNP L is localized uniformly in the nucleoplasm and enriched in perinucleolar structures,[13,14] which were later identified as SLM/Sam68 Nuclear Bodies, where hnRNP L interacts with Sam68.[15] Splicing targets of hnRNP L affect diverse processes, including tumorgenesis,[16,17] T-cell activation,[18-21] vasculogenesis,[22] and signal transduction.[23] HnRNP L also regulates its own expression by a negative feedback loop, in which it activates splicing of a poison exon that leads to nonsense-mediated mRNA decay (NMD) of the hnRNP L mRNA.[24] HnRNP L can regulate alternative splicing either as an activator or a repressor, and it is still unclear what determines its activity in each specific case. As recently shown, alternative splicing regulation of hnRNP L can be based on interference with splice site recognition.[25]

To address how the multiple functions of hnRNP L correlate with RNA binding, we made use of a powerful new approach: individual nucleotide resolution crosslinking and immunoprecipitation (iCLIP) combined with RNA-Seq.[26] This recent development of the basic CLIP method allows genome-wide mapping of all in vivo RNA-interaction sites at single-nucleotide resolution for any RNA-binding protein.[27] CLIP approaches have been applied to several factors, including Nova,[28] SRSF1,[29] and—combined with next-generation sequencing—to Nova,[30] RbFox2,[31] PTB,[32] HuR,[33] SRSF3/4,[34] and others (reviewed in refs. 35 and 36). By integrating the CLIP binding data with information on expression of splice isoforms, functional RNA

*Correspondence to: Albrecht Bindereif; Email: Albrecht.Bindereif@chemie.bio.uni-giessen.de
Submitted: 11/30/2013; Revised: 01/23/2014; Accepted: 01/24/2014
http://dx.doi.org/10.4161/rna.27991

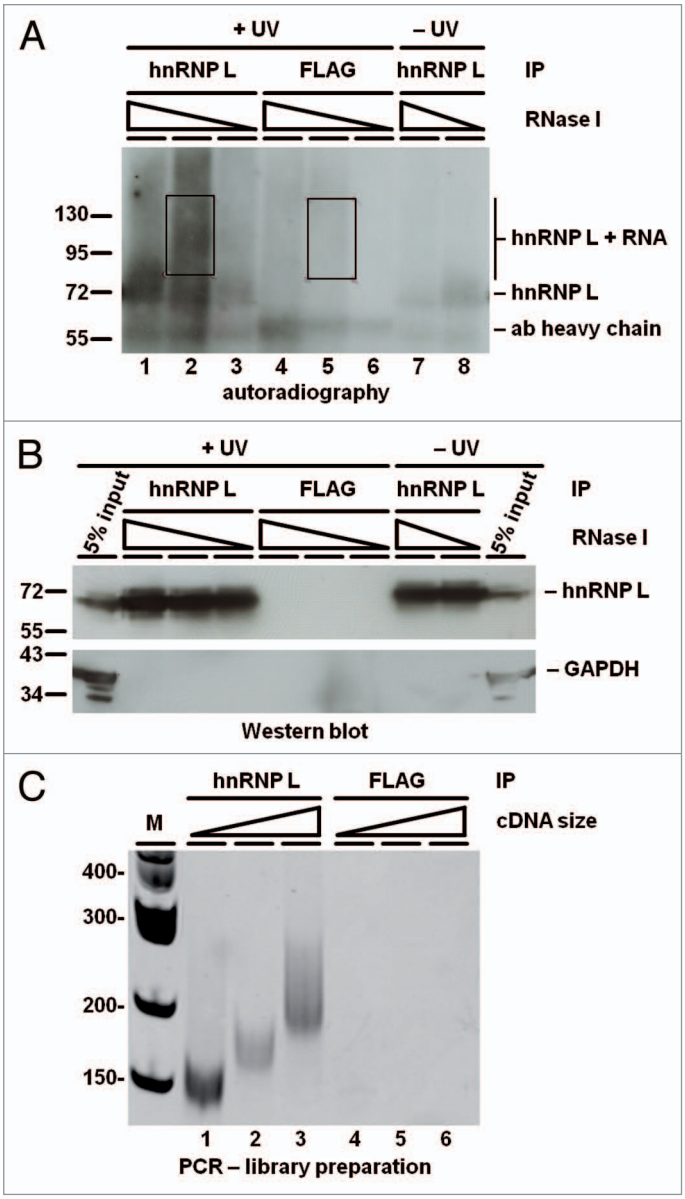

Figure 1. iCLIP-Seq analysis for transcriptome-wide mapping of hnRNP L RNA-binding sites. (**A**) A representative experiment is shown: Briefly, protein–RNA interactions were crosslinked by UV-irradiation of HeLa cells, followed by lysate preparation, limited RNase digestion, immunoprecipitation of hnRNP L-RNA adducts, 3′-RNA-linker addition to the RNA tags, 5′-terminal ^{32}P-labeling, and gel separation of the covalent RNA–protein complexes under denaturing conditions. Autoradiography of iCLIP membrane with bound ^{32}P-labeled RNA–protein complexes, comparing after UV-irradiation (+UV) hnRNP L- (lanes 1–3) with control FLAG immunoprecipitated material (IP, lanes 4–6). As additional control, UV irradiation was left out (lanes 7–8). In each case, different amounts of RNase I were applied (as indicated). Boxed regions were cut out and subjected to RNA isolation and library preparation. Marker positions and the mobilities of hnRNP L-RNA adducts, limit-digest hnRNP L, and of the antibody heavy chain are marked. (**B**) Western blot analysis of the same membrane as in panel (**A**), using anti-hnRNP L and GAPDH antibodies and including 5% input material. (**C**) Library preparation from iCLIP-processed hnRNP L- (IP; lanes 1–3) or control FLAG-immunoprecipitated material (FLAG-IP; lanes 4–6). PCR products for high-throughput sequencing were visualized by ethidium bromide staining on a 6% polyacrylamide-TBE gel. The three different size fractions resulted from prior size selection of the cDNA, following reverse transcription. PCR products derived from all three immunoprecipitations were pooled for sequencing.

maps can be derived that reveal position-dependent splicing effects.[26,37]

Based on iCLIP-Seq and genomic mapping, we obtained a comprehensive genome-wide map of hnRNP L RNA interaction sites in HeLa cells. Analysis of the crosslink sites revealed several novel regulatory roles of hnRNP L: First, hnRNP L RNA-binding follows distinct patterns for exons activated or repressed by hnRNP L, indicating a positional code and a predictive RNA map. Second, hnRNP L binding is enriched at both terminal as well as internal poly(A) sites. Third, hnRNP L binding preferentially overlaps with predicted miRNA target sites in the 3′ UTR, consistent with an hnRNP L-vs.-miRNA competition model. For a subset of these targets, we demonstrated 3′ UTR-depending translational regulation by hnRNP L. A very recent study has also investigated hnRNP L by CLIP-Seq in T-cells.[38] Although focusing on hnRNP L-regulated splicing changes specific to T-cell biology, remarkably similar results were obtained on target distribution and specificity (see Discussion).

Results and Discussion

HnRNP L in vivo RNA-crosslink sites determined by iCLIP match in vitro consensus

To monitor genome-wide RNA binding sites of hnRNP L in HeLa cells, we performed three iCLIP experiments, combined with Solexa high-throughput sequencing (for a representative experiment, see **Fig. 1**). Sequence reads from the three experiments were combined and analyzed for hnRNP L crosslink sites. Genomic mapping and sequence analysis was performed,[26] resulting in ~1.1 million sites mapped on chromosomes 1–22 and X (**Fig. S1A**; for details on data processing, see Supplementary Materials and Methods; for the high reproducibility between the three experiments, see **Fig. S1B**).

Sequence motif analysis (in pentamers, as described in ref. 39) revealed significant enrichment of CA-repeat and CA-rich motifs (**Fig. 2A**): CA-repeats (ACACA, CACAC) were enriched by about 110–140% (100% corresponding to a 2-fold enrichment) and certain CA-rich motifs by 80–95% (ACAT, TACA). This specific enrichment pattern perfectly agrees with hnRNP L-binding properties derived earlier by an in vitro SELEX study.[1] In contrast, the control experiment yielded no significant enrichment of a specific pentamer. Shankarling et al. (2014) obtained a similar binding consensus in their CLIP-Seq analysis.[38]

Activator vs. repressor function of hnRNP L in alternative splicing depends on its binding position

The ~1.1 million sites were clustered and filtered, and a total of 622789 crosslink sites were selected for functional analysis (see Supplementary Materials and Methods). **Figure 2B** presents the distribution of the crosslink sites: A large fraction (72.3%) of hnRNP L binding sites maps within protein-coding genes, particularly in their introns (40.5%) compared with the mRNA (31.8%). The relatively high number of crosslink sites in introns is striking, considering the transient nature of intronic sequences, suggesting a global regulatory role of hnRNP L through intron

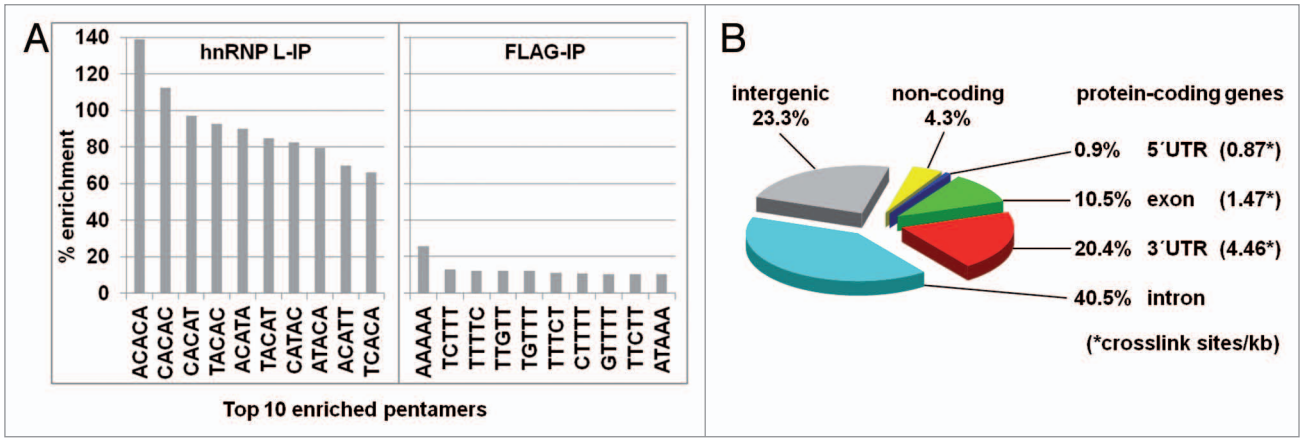

Figure 2. Genome-wide hnRNP L RNA-binding analysis by iCLIP. (**A**) Sequence motif analysis. HnRNP L crosslink sites were analyzed for motif enrichment (5-mers within a -30 to -10 and +10 to +30 window compared with 100 randomized positions from the same regions of the gene. The top 10 pentamers are listed for the hnRNP L- vs. the control FLAG immunoprecipitation (IP). All *P* values were < 0.01. (**B**) Distribution of hnRNP L crosslink sites, including their respective crosslink densities.

binding. Within mRNA transcripts, 3′ UTRs exhibit a much higher density of binding sites than exons (4.46 vs. 1.47 crosslink sites per kb), consistent with known functions of hnRNP L in the 3′ UTR (see Introduction). This binding distribution of hnRNP L on the genome-wide level as well as on pre-mRNA regions is similar to that observed in both primary and immortalized T-cells, no matter if activated or repressed.[38]

To investigate the RNA-binding patterns of hnRNP L near splice sites, we used all ENCODE-annotated exons of protein-coding genes and grouped their splice sites into two classes: alternative and constitutive. The frequency of crosslink sites around these two groups of splice sites is plotted in **Figure 3A**. The apparent overrepresentation of hnRNP L binding sites in constitutive exons most likely simply reflects their higher abundance. The discrete peaks at the 5′ splice site and at the -25 to -40 region relative to the 3′ splice site are probably not based on hnRNP L crosslink sites, but may reflect primer-extension stops at the branched lariat after RNase treatment, with hnRNP L bound to the respective intron. More interestingly, we detected a higher density of hnRNP L binding sites around alternative 5′ splice sites, compared with constitutive 5′ splice sites, both in the exonic (positions -30 to 0) and intronic regions (0 to +70); in addition, in the alternative 3′ splice site regions there are strikingly more hnRNP L binding sites around position -20. This pattern suggests that hnRNP L regulates splice site usage predominantly through binding around the 5′ splice site region, involving either exonic or intronic elements, and through binding within the pyrimidine tract region.

Next we correlated RNA-binding and alternative splicing targets: HnRNP L was downregulated in HeLa cells by RNAi, followed by an additional cycloheximide treatment to suppress nonsense-mediated RNA decay (NMD) and to detect premature termination codon-containing splice variants. Splice-sensitive exonarray and data analysis predicted 890 hnRNP L-activated and 574-repressed target cassette exons (see Supplementary Materials and Methods).

Based on these two data sets, we analyzed the density of hnRNP L crosslink sites, comparing activated vs. repressed exons (**Fig. 3B**). This revealed clear differences in hnRNP L binding around the splice sites: The repressor activity of hnRNP L concentrates immediately upstream of the 3′ splice site (peaking around position -40), whereas hnRNP L preferentially activates when bound at intronic positions further downstream of the 5′ splice site (positions +25 to +200). The apparent higher density in activated vs. repressed exons likely reflects their different abundances.

In sum, our data suggest that hnRNP L preferentially represses 3′ splice sites through interfering with the recognition of the pyrimidine tract/3′ splice site region, and around the 5′ splice site, and activates 5′ splice sites from downstream intronic positions. The binding position relative to the regulated exon therefore appears to provide an important determinant in specifying hnRNP L's activator and repressor function (schematically represented below **Fig. 3B**). In contrast, in a recent study focusing on alternative splicing of genes important in T-cell biology, no positional code was observed; most likely due to the much lower number of investigated hnRNP L-regulated splicing events.[38]

In fact, several examples of hnRNP L-mediated splicing regulation support our conclusions from this global analysis: First, hnRNP L as a splicing activator was initially discovered for the human *eNOS* gene, where an intronic CA-repeat region activates the 5′ splice site of the upstream exon 13.[40] Second, alternative exon 6 of the human *MAPK10* gene is strongly regulated by a CA-repeat enhancer (positions +61 to +118 of intron 6; ref. 1). Third, our initial exonarray analysis[10] provided several examples of hnRNP L repressing alternative exons by binding close to their 3′ splice site, which can be based on U2AF interference, as demonstrated for *TJP1*.[25] Additionally, hnRNP L binding in very close proximity to the 5′ splice site can interfere with recognition by the U1 snRNP, as shown for *SLC2A2*,[25] which is consistent with a minor effect in the RNA map at a region 0 to +25 relative to the 5′ splice site. Other splicing factors function by related mechanisms: CLIP analyses of Nova[28,30] and RBFOX2[31] revealed similar functional binding patterns as observed for hnRNP L, whereas PTB instead represses alternative exons also from

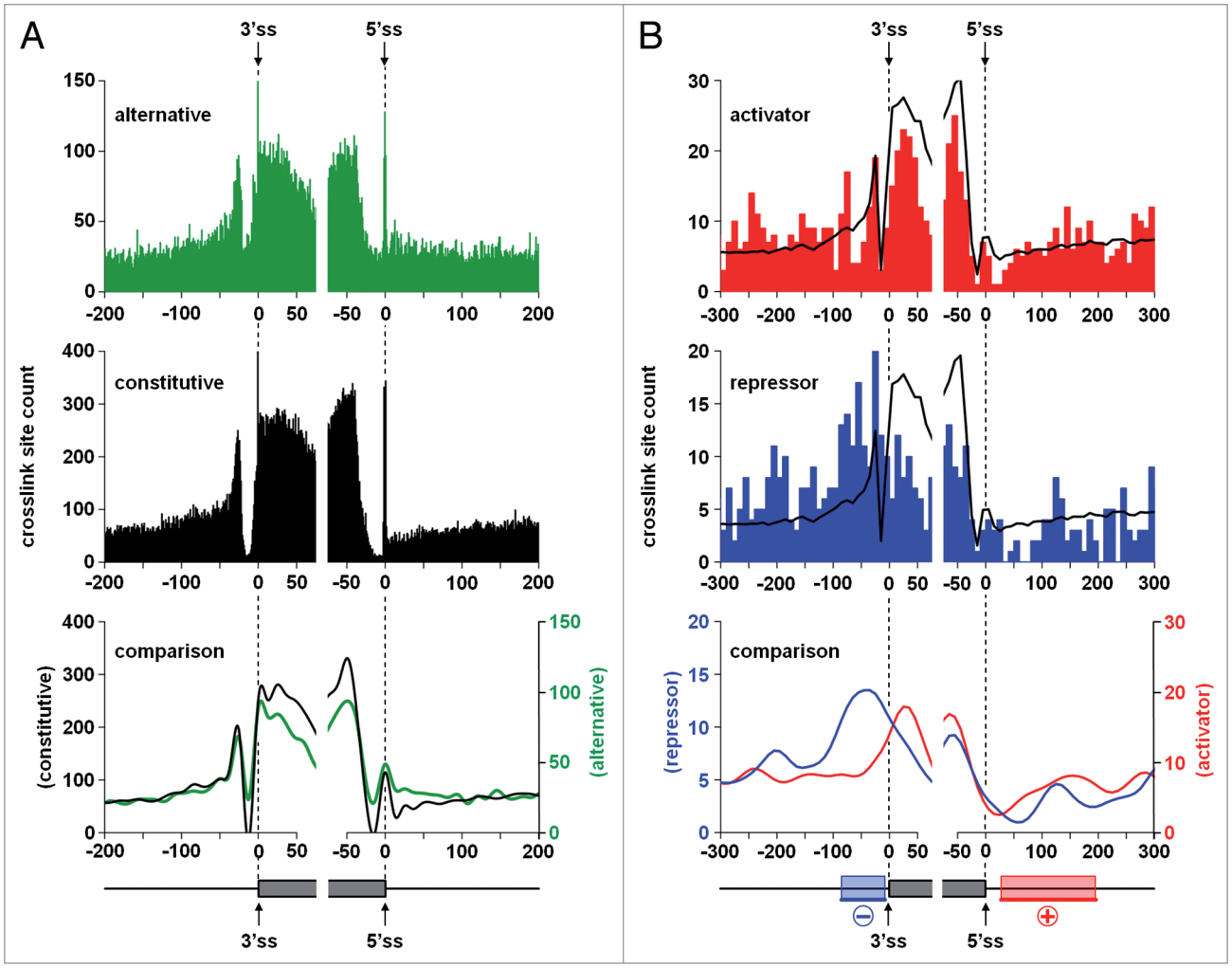

Figure 3. HnRNP L activates or represses alternative splicing in a position-dependent manner. (**A**) Number of hnRNP L crosslink sites around 3′ (-200 to +75) and 5′ splice sites (-75 to +200) of protein-coding genes is diagrammed, separately for alternative and constitutive splice sites (upper and middle panels, respectively). Below, alternative (green) and constitutive (black) splice sites are compared, plotted in smooth lines (lower panel). (**B**) Number of hnRNP L crosslink sites around 3′ (-300 to +75) and 5′ splice sites (-75 to +300) of hnRNP L-regulated exons, separately for activated (upper panel) and repressed exons (middle panel). Non-target exons were used as background (black smooth lines). In the lower panel, hnRNP L-activated (red) and -repressed exons (blue) exons are compared, plotted in smooth lines. Below, the positional information of hnRNP L binding and its correlation with activator/repressor function is schematically summarized.

downstream intronic positions, and activates by binding to the intron in close proximity to the flanking constitutive exons.[32] A recent study investigated six hnRNP proteins (A1, A2/B1, F, H1, M, and U) by CLIP-Seq.[41] Interestingly, in RNA maps derived from these data, hnRNP F and U activated exon inclusion from positions overlapping with hnRNP L repressor sites. In contrast, hnRNP A2/B1 and M repress alternative exons from hnRNP L's activator position, suggesting potential antagonistic mechanisms of hnRNP L and other hnRNPs in alternative splicing regulation.

There are other cases of complex alternative splicing mechanisms regulated by hnRNP L, involving co-regulators such as the paralog hnRNP L-like, for example, the case of the *CD45* gene.[18-21,42] In this mechanism, an interplay of both splicing factors regulates three differentially spliced exons of *CD45*, dependent on the activation state of different immune cells. Such mechanisms probably represent a special minority of events and cannot be accounted for in the presented RNA map. Also, since *CD45* is not expressed in HeLa cells, our iCLIP approach did not include it.

HnRNP L binding overlaps with polyadenylation signals

In addition to positional binding of hnRNP L around the splice sites, we investigated the crosslink-site density in proximity to polyadenylation [poly(A)] sites. All ENCODE-annotated polyadenylation events from protein-coding genes were grouped into terminal and internal poly(A) sites (**Fig. 4**), and the hnRNP L crosslink-site density was plotted in windows of -300 to +300 nucleotides relative to internal (top diagram, in red) and terminal poly(A) sites (middle diagram, in blue). The high crosslink-site density downstream of the poly(A) site in case of the internal poly(A) sites reflects hnRNP L binding in this region of the (pre-)mRNA. In contrast, hnRNP L binding disappeared downstream of terminal poly(A) sites, since most of the mRNA is cleaved. In both groups, the crosslink site frequency increased

toward the poly(A) site, up to a position around -30. The strongly reduced frequency of crosslink sites between position -30 and the poly(A) site is due to the alignment problem with short sequence reads containing poly(A) tails. Interestingly, this region contains important control elements for the poly(A) site recognition, such as the $AAUA_3$ signal, 15–30 nucleotides upstream of the poly(A) site, which is bound by CPSF; as well as a U-rich upstream sequence element (USE), which was shown to enhance polyadenylation (reviewed in ref. 43). This hnRNP L crosslink site distribution suggests that hnRNP L may commonly regulate poly(A) site selection through competing with binding of components of the polyadenylation machinery. Consistent with this we had previously described an example of hnRNP L-dependent alternative poly(A) site selection, based on an exonarray analysis after hnRNP L knockdown. In the *ASAH1* mRNA, an internal poly(A) site is more frequently used if hnRNP L is downregulated, indicating suppression of internal polyadenylation by hnRNP L.[10]

HnRNP L binds preferentially in close proximity to predicted miRNA binding sites in 3′ UTR and can thereby regulate translation efficiency

It has been recently reported that hnRNP L competes with miRNAs for binding to the *VEGFA* 3′ UTR in hypoxia, thereby modulating miRNA function.[11] Analyzing our iCLIP data, we in fact observed hnRNP L crosslink sites at a high density within and around these specific miRNA target sites. Interestingly, a second set of predicted miRNA-target sites overlapping with dense hnRNP L binding was observed in the downstream half of the *VEGFA* 3′ UTR (**Fig. 5A and B**). Since ~20% of hnRNP L crosslink sites were mapped to 3′ UTRs (**Fig. 2B**), competition of hnRNP L with miRNAs for binding to their respective target sites may represent a general mechanism.

To investigate this on a genome-wide level, we extracted the conserved mammalian miRNA target sites in the 3′ UTRs of RefSeq genes, as predicted by TargetScanHuman 5.1 (http://www.targetscan.org). We first determined the frequency of hnRNP L crosslink sites within a region of 80 nt up- and downstream of the target sites (**Fig. 5C**), confirming an increased frequency of hnRNP L crosslinks on and around miRNA target sites.

Second, we compared the density of hnRNP L crosslinks at the miRNA target sites (positions -20 to +20 of target sites) vs. outside of the miRNA target sites (**Fig. 5D**), based on 5062 3′ UTRs that contain both crosslink sites and miRNA target sites (see Supplementary Materials and Methods). We conclude that the density at the miRNA target sites is significantly higher than outside, suggesting that competition of hnRNP L with binding of the Ago/miRNA complexes provides a global mechanism of hnRNP L function.

To predict potential target mRNAs for such a regulatory mechanism, two strategies were applied. First, dense hnRNP L binding clusters (based on our iCLIP data) were screened for overlap with TargetScan-predicted miRNA binding sites of miRNAs expressed in HeLa cells.[44] Second, the top Ago2 binding clusters (based on PAR-CLIP[45]) were screened for overlap with dense hnRNP L binding clusters and TargetScan-predicted miRNA binding sites. As a result, 16 potential target genes were derived

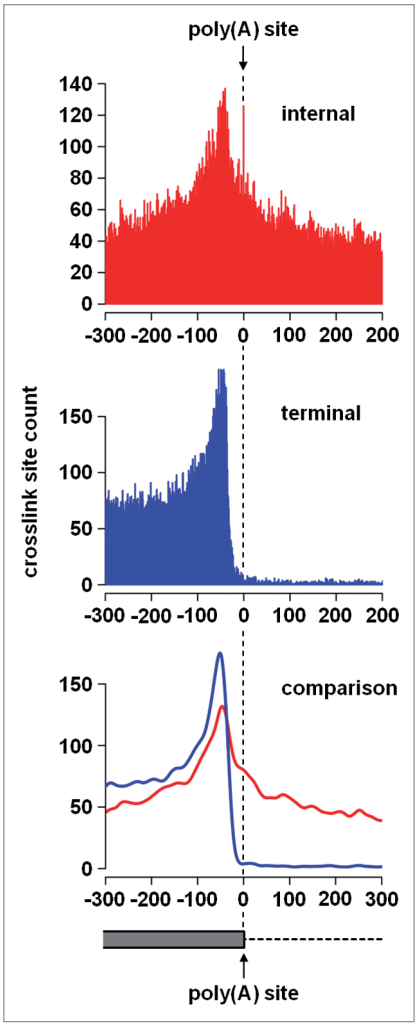

Figure 4. HnRNP L binding overlaps with polyadenylation signals. Number of hnRNP L crosslink sites around polyadenylation [poly(A)] sites (positions -300 to +300) of protein-coding genes is diagrammed, separately for internal and terminal poly(A) sites (upper and lower panels, respectively). Below, internal (red) and terminal (blue) poly(A) sites are compared, plotted in smooth lines after normalization (lower panel).

(**Fig. S2**). Since hnRNP L was reported to be involved in mRNA stability, either by destabilizing (*SLC2A1* mRNA[4]) or by stabilizing (*BCL2* mRNA[9]), in each case by binding to a CA-rich region in the 3′ UTR, we assayed by quantitative RT-PCR the steady-state mRNA levels of the 16 mRNAs after hnRNP L knockdown (**Fig. 6A and B**). Only in two cases (*GNG5* and *DAB2*), steady-state mRNA levels were significantly increased after hnRNP L knockdown, suggesting a destabilizing role of hnRNP L (as in *SLC2A1* mRNA[4]). However, hnRNP L binding in the 3′ UTR does not appear to be a widespread determinant of mRNA stability in this set of predicted target mRNAs.

To analyze potential effects of altered hnRNP L levels on translation efficiency, six selected 3′ UTR regions containing both hnRNP L crosslink and predicted miRNA binding sites (*DAB2*, *HNRNPK*, *KPNB1*, *LDHB*, and two different regions from *LAPTM4A*; **Fig. S2E, F, J, and O**) were cloned in the 3′ UTR of a firefly luciferase reporter. Note that hnRNP L levels change

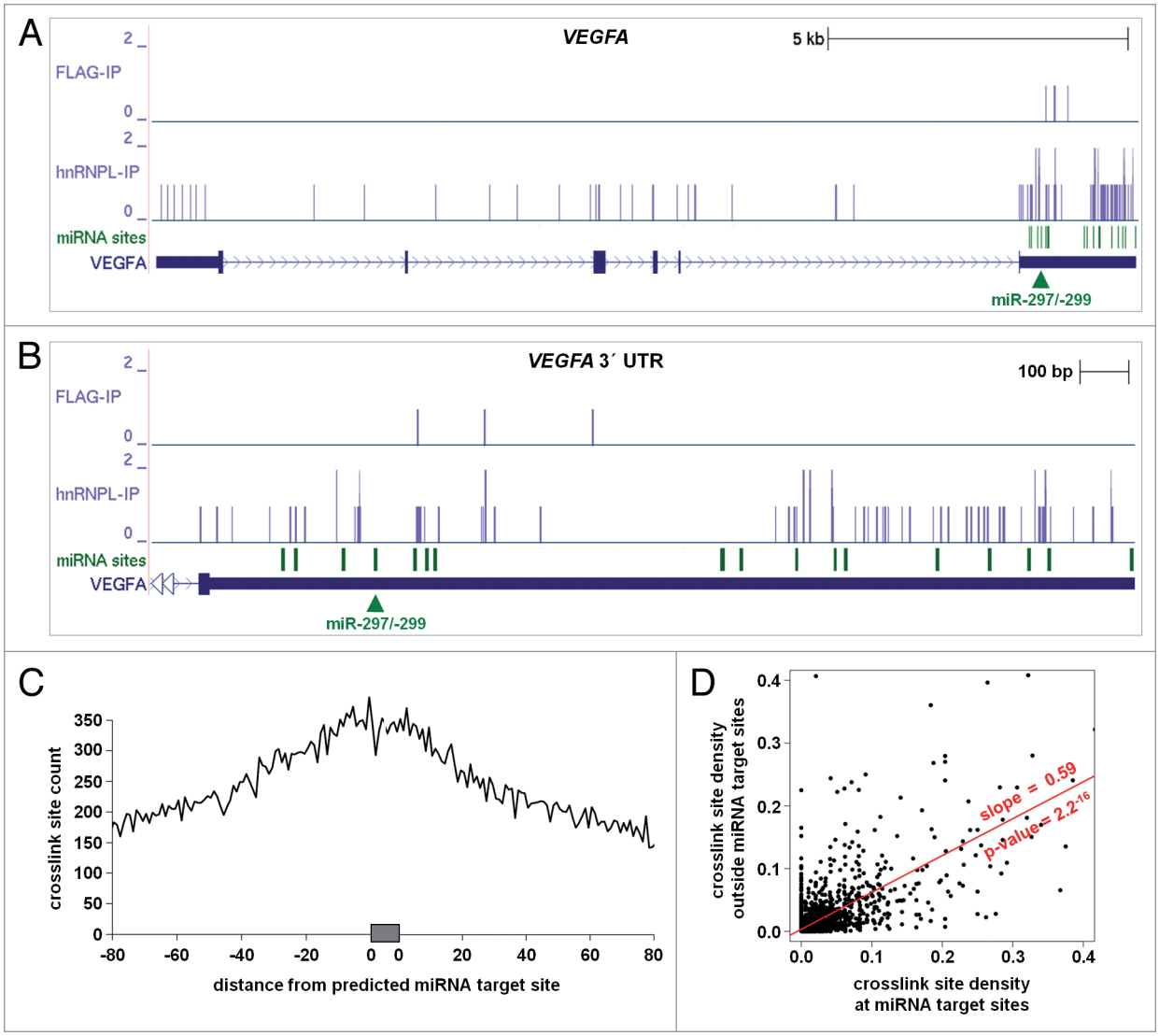

Figure 5. HnRNP L binds preferentially to miRNA target sites in 3′ UTRs. (**A**) UCSC Genome Browser view of *VEGFA* exon/intron structure with crosslink-site distribution determined by iCLIP (hnRNP L-IP vs. control FLAG-IP). The middle panel (miRNA sites; in green) shows conserved mammalian miRNA regulatory target sites for conserved miRNA families in the 3′ UTR regions of Refseq genes, as predicted by 'TargetScanHuman 5.1' (http://www.targetscan.org). Target sites of miR-297 and miR-299, where hnRNP L modulates miRNA repression are highlighted by a green arrowhead below.[11] (**B**) UCSC Genome Browser view of the *VEGFA* 3′ UTR, represented as in panel (**A**). (**C**) Frequency of crosslink sites around predicted miRNA target sites (-80 to +80 of target site). (**D**) Comparison of the crosslink site density between miRNA target site regions (from position -20 to +20 relative to the miRNA target site, including the miRNA target site itself) on the X-axis, and the corresponding non-target regions on the Y-axis, based on 3′ UTRs of 5062 protein-coding genes that contain both miRNA target sites and crosslink sites.

both in the nucleus as well as, more importantly, in the cytoplasm (**Fig. 6C**). The luciferase constructs and a control without 3′ UTR insertion were transfected in HeLa cells, where hnRNP L levels had been increased by overexpression or decreased by siRNA-mediated knockdown (**Fig. 6D**). In five of the six constructs tested (*DAB2*, *HNRNPK*, *KPNB1*, *LAPTM4A* region 1 and 2) translation efficiency significantly decreased after hnRNP L knockdown; in two cases (*HNRNPK* and one of the *LAPTM4A* 3′ UTRs) translation efficiency increased after hnRNP L overexpression (**Fig. 6E**). The reciprocal effects in these two cases are consistent with a model, whereby hnRNP L competes with miRNA/Ago binding to target 3′ UTRs, as previously shown for the *VEGFA* mRNA.[11] Why do we see only two cases of reciprocal, hnRNP L-dependent effects on translation, and in the other three constructs (*DAB2*, *KPNB1*, and *LAPTM4A*.2) only a decrease in translation efficiency upon hnRNP L knockdown? We know that hnRNP L levels in the cytoplasm are lower than in the nucleus (ref. 10; **Fig. 6C**), yet most likely these effects depend on the relative steady-state levels of hnRNP L as well as of the respective miRNA and target 3′ UTR. Of these targets, the *HNRNPK* mRNA is particularly interesting, since hnRNP proteins are often tightly linked in their expression by cross-regulatory networks.

A recent study pointed to the cross-regulatory relationships between hnRNP proteins.[41] Interestingly, hnRNP L binding

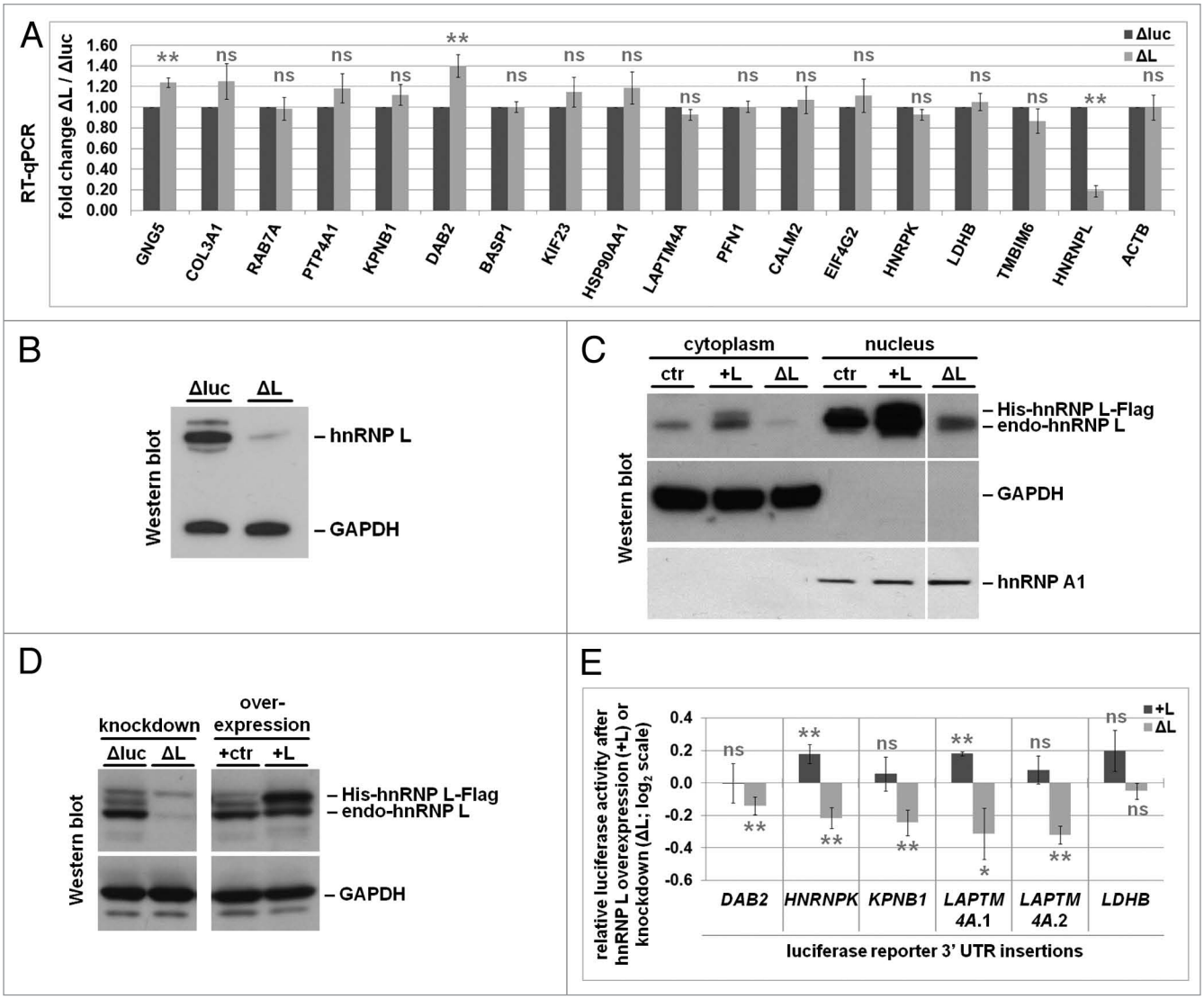

Figure 6. HnRNP L knockdown and overexpression affects translational efficiency of luciferase reporters bearing 3′ UTRs with predicted hnRNP L/miRNA binding sites. (**A**) Steady-state mRNA levels of predicted hnRNP L/miRNA targets after hnRNP L knockdown. Total RNA was isolated from hnRNP L knockdown (ΔL) and luciferase control knockdown (Δluc) cells (see panel **B**), and subjected to quantitative RT-PCR analysis with gene-specific PCR primers against the 16 potential target mRNAs (as indicated). *HNRNPL*- and *ACTB*-specific primers served as controls; samples were normalized to U1 snRNA. Student's *t* test was performed (**: *P* value < 0.01; *: *P* value = 0.01–0.05; ns: not significant, *P* value > 0.05). (**B**) Representative western blot of siRNA-mediated hnRNP L knockdown (ΔL) and luciferase control knockdown (Δluc), using antibodies against hnRNP L and GAPDH (loading control). (**C**) HnRNP L protein levels upon knockdown or overexpression change correspondingly both in the nucleus and in the cytoplasm. HeLa cells were transfected with an siRNA against hnRNP L (ΔL) or a vector expressing His-/Flag-tagged hnRNP L (+L) and compared with control cells (ctr). Nuclear and cytoplasmic extracts were prepared, followed by western blot analysis with antibodies against hnRNP L, detecting both endogenous (endo-hnRNP L) and the overexpressed tagged protein (His-hnRNP L-Flag); GAPDH served as a cytoplasmic, hnRNPA1 as a nuclear marker. Note that although hnRNP A1 is a shuttling protein, its steady-state levels are much higher in the nucleus, with the cytoplasmic levels below the detection limit under these conditions. (**D and E**) Effects of hnRNP L knockdown or overexpression on luciferase reporter expression. To test for effects of hnRNP L knockdown, cells were transfected with either an unrelated luciferase-control siRNA (Δluc) or an hnRNP L-specific siRNA (ΔL); to test for effects on hnRNP L overexpression, an empty vector control (+ctr) or a vector expressing His/Flag-tagged hnRNP L protein (+L) were transfected, always in addition to a dual luciferase reporter construct expressing both firefly luciferase with or without selected 3′ UTR insertions, using Renilla luciferase for normalization. Lysates were prepared, followed by western blot analysis with antibodies against hnRNP L, detecting both endogenous (endo-hnRNP L) and the overexpressed tagged protein (His-hnRNP L-Flag), as well as GAPDH as a loading control (panel **D**). Firefly luciferase activity of reporters with 3′ UTR insertions (as indicated) was monitored (panel **E**), normalized to Renilla luciferase activity in the same lysate, comparing the effects of hnRNP L knockdown (ΔL) and overexpression (+L). The 3′ UTR regions selected are marked as red boxes in **Figure S2**. The fold changes between hnRNP L knockdown/overexpression and the respective control were calculated, normalized to a firefly luciferase reporter without 3′ UTR insertion, and displayed as $\log_2$ values. All values and standard deviations were derived from three biological replicates. Student's *t* test was performed, comparing relative luciferase activity from the cells expressing the reporter without 3′ UTR insertion (reference) to the respective 3′ UTR insert-carrying reporters (**, *P* value < 0.01; *, *P* value = 0.01–0.05; ns, not significant, *P* value > 0.05).

clusters are also found in the 3′ UTRs of hnRNP A1, A2/B1, F, H1, M, and U, in each case overlapping with predicted miRNA target sites (data not shown). We conclude that an hnRNP L/miRNA-competition mechanism may add another layer of complexity to the cross-regulatory networks between hnRNP proteins.

Materials and Methods

iCLIP, sequencing, and genomic mapping

Three individual iCLIP experiments were performed with HeLa cells, using hnRNP L-specific antibody 4D11 (Sigma), and FLAG antibody (Sigma M2) as a negative control, followed by sequencing on an Illumina GAIIx sequencer (50 bp single-end reads). For experimental procedures and genomic mapping, see reference 26.

Statistics and bioinformatics

Data analysis details are described in the Supplementary Materials and Methods, sections 1–7. Solexa sequencing reads (.fastq files) of iCLIP experiments and filtered crosslink sites combining all three experiments of hnRNPL (hnRNPL_crosslink_site.bed) were deposited to the NCBI GEO database (GSE 37562), as well as exon array raw data (.CEL files) of hnRNP L-knockdown experiments and lists of regulated exons predicted to be activated (activated_exon.txt) or repressed (repressed_exon.txt) by hnRNP L.

hnRNP L knockdown and RT-PCR analysis

Knockdown of hnRNP L in HeLa cells was performed for four days as described earlier,[10] with two different siRNAs against hnRNP L or Luciferase as a control. To monitor hnRNP L knockdown on the protein level, western blotting was performed as described below. Total RNA was isolated using TRIzol reagent (Invitrogen) and RNeasy columns (QIAGEN). RNA was reverse-transcribed (iScript cDNA Synthesis Kit, Bio-Rad) and specific mRNAs were monitored by semiquantitative PCR. For primer and siRNA sequences, see Supplementary Materials and Methods (section 8). For quantitative PCR, cDNAs were measured with the KAPA SYBR FAST QPCR MasterMix (PeqLab) in a Mastercycler ep realplex^2 S (Eppendorf). Relative RNA levels from three biological and three technical replicates each were calculated according to Pfaffl (2001).[46]

HnRNP L overexpression and subcellular fractionation

To control whether cytoplasmic hnRNP L levels change after knockdown or overexpression, siRNA-mediated knockdown was performed as described above, or His/Flag-tagged hnRNP L was overexpressed,[24] using pcDNA3-His-hnRNP L-Flag, followed by subcellular fractionation (ProteoJET Cytoplasmic and Nuclear Protein Extraction Kit, Fermentas). Cytoplasmic and nuclear extracts were subjected to western blot analysis with hnRNP L 4D11 (Sigma), GAPDH 6C5 (Ambion), and hnRNP A1 4B10 (Santa Cruz) antibodies, using the Lumi-Light Western Blotting Substrate (Roche).

Firefly luciferase/3′ UTR constructs and luciferase reporter assays

3′ UTR regions from selected genes (indicated by red boxes in **Fig. S2**) were PCR-amplified, and products were cloned into the multiple cloning site of pmirGLO Dual-Luciferase miRNA Target Expression Vector (Promega), within the 3′ UTR of the firefly luciferase reporter gene and between SalI and *Sac*I restriction sites.

For the luciferase reporter assay in combination with hnRNP L knockdown, 3.8×10^4 HeLa cells per well were reverse-transfected in a 12-well plate, using siRNA at a final concentration of 12.5 nM in culture medium (hnRNP L 3′-UTR or luciferase GL2) and 2.1 µl Lipofectamine RNAiMAX Reagent in 210 µl OptiMEM medium (both Life Technologies). Note that no binding sites for luciferase GL2 siRNA are contained in firefly or Renilla luciferase reporters within pmirGLO. After hnRNP L knockdown for three days, the cells were transfected with 1 µg of the pmirGLO reporter plasmids (with or without 3′ UTR insertion), diluted in 41 µl OptiMEM medium and 2.9 µl FuGENE HD Transfection Reagent (Promega). Cells were further incubated for 24 h.

For the luciferase reporter assay in combination with hnRNP L overexpression, 1.14×10^5 HeLa cells per well were seeded the day before transfection in a 12-well plate. 230 ng of empty pcDNA3 vector or pcDNA3-His-hnRNP L-Flag vector were transfected in combination with 910 ng of the pmirGLO reporter plasmids (with or without 3′ UTR insertion), diluted in 114 µl OptiMEM medium, using 2.3 µl TurboFect Transfection Reagent (Thermo Scientific), and incubated for 24 h. Cells were lysed by adding 200 µl Lysis-Juice 2 (PJK), following the manufacturer's instructions. An aliquot of these lysates was analyzed by western blotting as described above to verify hnRNP L knockdown/overexpression. Bioluminescence was monitored for firefly luciferase, using Beetle-Juice Kit, and for Renilla luciferase, using Renilla-Juice Kit (both PJK) in an Orion L Microplate Luminometer (Titertek-Berthold).

Disclosure of Potential Conflicts of Interest

No potential conflicts of interest were disclosed.

Acknowledgments

We thank Julia Renz for transfection, cell fractionation, and western blot assays, Lorraine Fischer, Sina Fuchs, and Melanie Goebel for construction of the luciferase reporter constructs, and Marcel Oschwald for western blots. This work was supported by grants from the Deutsche Forschungsgemeinschaft (Bi 316/12, IRTG1384, and a German-Israeli Project Cooperation Grant, to AB), the Federal Ministry for Education and Research (BMBF RUS 10/030; to Bindereif A and Gelfand MS), the European-Commission-funded Network of Excellence EURASNET (to Bindereif A), Russian State contract 14.740.11.0003 (to Gelfand MS), the Slovenian Research Agency (P2-0209, Z7-3665; to Curk T and Zupan B), and the Russian Academy of Sciences (programs Molecular and Cellular Biology and Basic Medical Science; to Gelfand MS). The results in this work are part of a dissertation (Oliver Rossbach) submitted at the Justus Liebig University in Giessen.

Supplemental Materials

Supplemental materials may be found here:
http://www.landesbioscience.com/journals/rnabiology/article/27991/

References

1. Hui J, Hung LH, Heiner M, Schreiner S, Neumüller N, Reither G, Haas SA, Bindereif A. Intronic CA-repeat and CA-rich elements: a new class of regulators of mammalian alternative splicing. EMBO J 2005; 24:1988-98; PMID:15889141; http://dx.doi.org/10.1038/sj.emboj.7600677
2. Liu X, Mertz JE. HnRNP L binds a cis-acting RNA sequence element that enables intron-dependent gene expression. Genes Dev 1995; 9:1766-80; PMID:7542615; http://dx.doi.org/10.1101/gad.9.14.1766
3. Guang S, Felthauser AM, Mertz JE. Binding of hnRNP L to the pre-mRNA processing enhancer of the herpes simplex virus thymidine kinase gene enhances both polyadenylation and nucleocytoplasmic export of intronless mRNAs. Mol Cell Biol 2005; 25:6303-13; PMID:16024770; http://dx.doi.org/10.1128/MCB.25.15.6303-6313.2005
4. Hamilton BJ, Nichols RC, Tsukamoto H, Boado RJ, Pardridge WM, Rigby WF. hnRNP A2 and hnRNP L bind the 3'UTR of glucose transporter 1 mRNA and exist as a complex in vivo. Biochem Biophys Res Commun 1999; 261:646-51; PMID:10441480; http://dx.doi.org/10.1006/bbrc.1999.1040
5. Hahm B, Kim YK, Kim JH, Kim TY, Jang SK. Heterogeneous nuclear ribonucleoprotein L interacts with the 3′ border of the internal ribosomal entry site of hepatitis C virus. J Virol 1998; 72:8782-8; PMID:9765422
6. Majumder M, Yaman I, Gaccioli F, Zeenko VV, Wang C, Caprara MG, Venema RC, Komar AA, Snider MD, Hatzoglou M. The hnRNA-binding proteins hnRNP L and PTB are required for efficient translation of the Cat-1 arginine/lysine transporter mRNA during amino acid starvation. Mol Cell Biol 2009; 29:2899-912; PMID:19273590; http://dx.doi.org/10.1128/MCB.01774-08
7. Hwang B, Lim JH, Hahm B, Jang SK, Lee SW. hnRNP L is required for the translation mediated by HCV IRES. Biochem Biophys Res Commun 2009; 378:584-8; PMID:19061868; http://dx.doi.org/10.1016/j.bbrc.2008.11.091
8. Shih SC, Claffey KP. Regulation of human vascular endothelial growth factor mRNA stability in hypoxia by heterogeneous nuclear ribonucleoprotein L. J Biol Chem 1999; 274:1359-65; PMID:9880507; http://dx.doi.org/10.1074/jbc.274.3.1359
9. Lee DH, Lim MH, Youn DY, Jung SE, Ahn YS, Tsujimoto Y, Lee JH. hnRNP L binds to CA repeats in the 3'UTR of bcl-2 mRNA. Biochem Biophys Res Commun 2009; 382:583-7; PMID:19298794; http://dx.doi.org/10.1016/j.bbrc.2009.03.069
10. Hung LH, Heiner M, Hui J, Schreiner S, Benes V, Bindereif A. Diverse roles of hnRNP L in mammalian mRNA processing: a combined microarray and RNAi analysis. RNA 2008; 14:284-96; PMID:18073345; http://dx.doi.org/10.1261/rna.725208
11. Jafarifar F, Yao P, Eswarappa SM, Fox PL. Repression of VEGFA by CA-rich element-binding microRNAs is modulated by hnRNP L. EMBO J 2011; 30:1324-34; PMID:21343907; http://dx.doi.org/10.1038/emboj.2011.38
12. Kefas B, Floyd DH, Comeau L, Frisbee A, Dominguez C, Dipierro CG, Guessous F, Abounader R, Purow B. A miR-297/hypoxia/DGK-α axis regulating glioblastoma survival. Neuro Oncol 2013; 15:1652-63; PMID:24158111; http://dx.doi.org/10.1093/neuonc/not118
13. Piñol-Roma S, Swanson MS, Gall JG, Dreyfuss G. A novel heterogeneous nuclear RNP protein with a unique distribution on nascent transcripts. J Cell Biol 1989; 109:2575-87; PMID:2687284; http://dx.doi.org/10.1083/jcb.109.6.2575
14. Huang S. Review: perinucleolar structures. J Struct Biol 2000; 129:233-40; PMID:10806073; http://dx.doi.org/10.1006/jsbi.2000.4247
15. Rajan P, Dalgliesh C, Bourgeois CF, Heiner M, Emami K, Clark EL, Bindereif A, Stevenin J, Robson CN, Leung HY, et al. Proteomic identification of heterogeneous nuclear ribonucleoprotein L as a novel component of SLM/Sam68 Nuclear Bodies. BMC Cell Biol 2009; 10:82; PMID:19912651; http://dx.doi.org/10.1186/1471-2121-10-82
16. Dery KJ, Gaur S, Gencheva M, Yen Y, Shively JE, Gaur RK. Mechanistic control of carcinoembryonic antigen-related cell adhesion molecule-1 (CEACAM1) splice isoforms by the heterogeneous nuclear ribonuclear proteins hnRNP L, hnRNP A1, and hnRNP M. J Biol Chem 2011; 286:16039-51; PMID:21398516; http://dx.doi.org/10.1074/jbc.M110.204057
17. Goehe RW, Shultz JC, Murudkar C, Usanovic S, Lamour NF, Massey DH, Zhang L, Camidge DR, Shay JW, Minna JD, et al. hnRNP L regulates the tumorigenic capacity of lung cancer xenografts in mice via caspase-9 pre-mRNA processing. J Clin Invest 2010; 120:3923-39; PMID:20972334; http://dx.doi.org/10.1172/JCI43552
18. Motta-Mena LB, Heyd F, Lynch KW. Context-dependent regulatory mechanism of the splicing factor hnRNP L. Mol Cell 2010; 37:223-34; PMID:20122404; http://dx.doi.org/10.1016/j.molcel.2009.12.027
19. Melton AA, Jackson J, Wang J, Lynch KW. Combinatorial control of signal-induced exon repression by hnRNP L and PSF. Mol Cell Biol 2007; 27:6972-84; PMID:17664280; http://dx.doi.org/10.1128/MCB.00419-07
20. Tong A, Nguyen J, Lynch KW. Differential expression of CD45 isoforms is controlled by the combined activity of basal and inducible splicing-regulatory elements in each of the variable exons. J Biol Chem 2005; 280:38297-304; PMID:16172127; http://dx.doi.org/10.1074/jbc.M508123200
21. Rothrock CR, House AE, Lynch KW. HnRNP L represses exon splicing via a regulated exonic splicing silencer. EMBO J 2005; 24:2792-802; PMID:16001081; http://dx.doi.org/10.1038/sj.emboj.7600745
22. Ray PS, Jia J, Yao P, Majumder M, Hatzoglou M, Fox PL. A stress-responsive RNA switch regulates VEGFA expression. Nature 2009; 457:915-9; PMID:19098893; http://dx.doi.org/10.1038/nature07598
23. Yu J, Hai Y, Liu G, Fang T, Kung SKP, Xie J. The heterogeneous nuclear ribonucleoprotein L is an essential component in the Ca2+/calmodulin-dependent protein kinase IV-regulated alternative splicing through cytidine-adenosine repeats. J Biol Chem 2009; 284:1505-13; PMID:19017650; http://dx.doi.org/10.1074/jbc.M805113200
24. Rossbach O, Hung LH, Schreiner S, Grishina I, Heiner M, Hui J, Bindereif A. Auto- and cross-regulation of the hnRNP L proteins by alternative splicing. Mol Cell Biol 2009; 29:1442-51; PMID:19124611; http://dx.doi.org/10.1128/MCB.01689-08
25. Heiner M, Hui J, Schreiner S, Hung LH, Bindereif A. HnRNP L-mediated regulation of mammalian alternative splicing by interference with splice site recognition. RNA Biol 2010; 7:56-64; PMID:19946215; http://dx.doi.org/10.4161/rna.7.1.10402
26. König J, Zarnack K, Rot G, Curk T, Kayikci M, Zupan B, Turner DJ, Luscombe NM, Ule J. iCLIP reveals the function of hnRNP particles in splicing at individual nucleotide resolution. Nat Struct Mol Biol 2010; 17:909-15; PMID:20601959; http://dx.doi.org/10.1038/nsmb.1838
27. Ule J, Jensen K, Mele A, Darnell RB. CLIP: a method for identifying protein-RNA interaction sites in living cells. Methods 2005; 37:376-86; PMID:16314267; http://dx.doi.org/10.1016/j.ymeth.2005.07.018
28. Ule J, Stefani G, Mele A, Ruggiu M, Wang X, Taneri B, Gaasterland T, Blencowe BJ, Darnell RB. An RNA map predicting Nova-dependent splicing regulation. Nature 2006; 444:580-6; PMID:17065982; http://dx.doi.org/10.1038/nature05304
29. Sanford JR, Coutinho P, Hackett JA, Wang X, Ranahan W, Caceres JF. Identification of nuclear and cytoplasmic mRNA targets for the shuttling protein SF2/ASF. PLoS One 2008; 3:e3369; PMID:18841201; http://dx.doi.org/10.1371/journal.pone.0003369
30. Licatalosi DD, Mele A, Fak JJ, Ule J, Kayikci M, Chi SW, Clark TA, Schweitzer AC, Blume JE, Wang X, et al. HITS-CLIP yields genome-wide insights into brain alternative RNA processing. Nature 2008; 456:464-9; PMID:18978773; http://dx.doi.org/10.1038/nature07488
31. Yeo GW, Coufal NG, Liang TY, Peng GE, Fu XD, Gage FH. An RNA code for the FOX2 splicing regulator revealed by mapping RNA-protein interactions in stem cells. Nat Struct Mol Biol 2009; 16:130-7; PMID:19136955; http://dx.doi.org/10.1038/nsmb.1545
32. Xue Y, Zhou Y, Wu T, Zhu T, Ji X, Kwon YS, Zhang C, Yeo G, Black DL, Sun H, et al. Genome-wide analysis of PTB-RNA interactions reveals a strategy used by the general splicing repressor to modulate exon inclusion or skipping. Mol Cell 2009; 36:996-1006; PMID:20064465; http://dx.doi.org/10.1016/j.molcel.2009.12.003
33. Lebedeva S, Jens M, Theil K, Schwanhäusser B, Selbach M, Landthaler M, Rajewsky N. Transcriptome-wide analysis of regulatory interactions of the RNA-binding protein HuR. Mol Cell 2011; 43:340-52; PMID:21723171; http://dx.doi.org/10.1016/j.molcel.2011.06.008
34. Änkö ML, Müller-McNicoll M, Brandl H, Curk T, Gorup C, Henry I, Ule J, Neugebauer KM. The RNA-binding landscapes of two SR proteins reveal unique functions and binding to diverse RNA classes. Genome Biol 2012; 13:R17; PMID:22436691; http://dx.doi.org/10.1186/gb-2012-13-3-r17
35. Milek M, Wyler E, Landthaler M. Transcriptome-wide analysis of protein-RNA interactions using high-throughput sequencing. Semin Cell Dev Biol 2012; 23:206-12; PMID:22212136; http://dx.doi.org/10.1016/j.semcdb.2011.12.001
36. König J, Zarnack K, Luscombe NM, Ule J. Protein-RNA interactions: new genomic technologies and perspectives. Nat Rev Genet 2011; 13:77-83; PMID:22251872; http://dx.doi.org/10.1038/nrg3141
37. Mukherjee N, Corcoran DL, Nusbaum JD, Reid DW, Georgiev S, Hafner M, Ascano M Jr., Tuschl T, Ohler U, Keene JD. Integrative regulatory mapping indicates that the RNA-binding protein HuR couples pre-mRNA processing and mRNA stability. Mol Cell 2011; 43:327-39; PMID:21723170; http://dx.doi.org/10.1016/j.molcel.2011.06.007
38. Shankarling G, Cole BS, Mallory MJ, Lynch KW. Transcriptome-wide RNA interaction profiling reveals physical and functional targets of hnRNP L in human T cells. Mol Cell Biol 2014; 34:71-83; PMID:24164894; http://dx.doi.org/10.1128/MCB.00740-13
39. Wang Z, Kayikci M, Briese M, Zarnack K, Luscombe NM, Rot G, Zupan B, Curk T, Ule J. iCLIP predicts the dual splicing effects of TIA-RNA interactions. PLoS Biol 2010; 8:e1000530; PMID:21048981; http://dx.doi.org/10.1371/journal.pbio.1000530
40. Hui J, Stangl K, Lane WS, Bindereif A. HnRNP L stimulates splicing of the eNOS gene by binding to variable-length CA repeats. Nat Struct Biol 2003; 10:33-7; PMID:12447348; http://dx.doi.org/10.1038/nsb875

41. Huelga SC, Vu AQ, Arnold JD, Liang TY, Liu PP, Yan BY, Donohue JP, Shiue L, Hoon S, Brenner S, et al. Integrative genome-wide analysis reveals cooperative regulation of alternative splicing by hnRNP proteins. Cell Rep 2012; 1:167-78; PMID:22574288; http://dx.doi.org/10.1016/j.celrep.2012.02.001
42. Preussner M, Schreiner S, Hung LH, Porstner M, Jäck HM, Benes V, Rätsch G, Bindereif A. HnRNP L and L-like cooperate in multiple-exon regulation of CD45 alternative splicing. Nucleic Acids Res 2012; 40:5666-78; PMID:22402488; http://dx.doi.org/10.1093/nar/gks221
43. Proudfoot NJ. Ending the message: poly(A) signals then and now. Genes Dev 2011; 25:1770-82; PMID:21896654; http://dx.doi.org/10.1101/gad.17268411
44. Landgraf P, Rusu M, Sheridan R, Sewer A, Iovino N, Aravin A, Pfeffer S, Rice A, Kamphorst AO, Landthaler M, et al. A mammalian microRNA expression atlas based on small RNA library sequencing. Cell 2007; 129:1401-14; PMID:17604727; http://dx.doi.org/10.1016/j.cell.2007.04.040
45. Hafner M, Landthaler M, Burger L, Khorshid M, Hausser J, Berninger P, Rothballer A, Ascano M Jr., Jungkamp AC, Munschauer M, et al. Transcriptome-wide identification of RNA-binding protein and microRNA target sites by PAR-CLIP. Cell 2010; 141:129-41; PMID:20371350; http://dx.doi.org/10.1016/j.cell.2010.03.009
46. Pfaffl MW. A new mathematical model for relative quantification in real-time RT-PCR. Nucleic Acids Res 2001; 29:e45; PMID:11328886; http://dx.doi.org/10.1093/nar/29.9.e45